

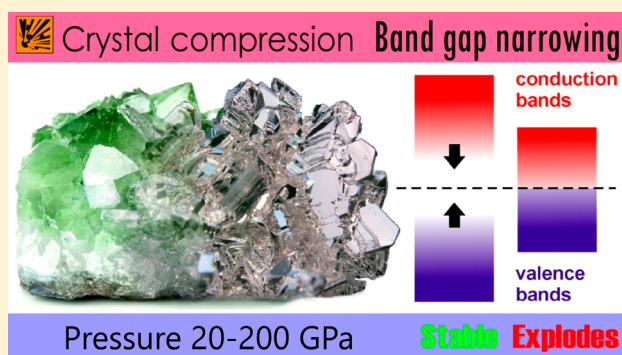
Quantification of Impact Sensitivity Based on Solid-State Derived Criteria

Sergey V. Bondarchuk*¹

Department of Chemistry and Nanomaterials Science, Bogdan Khmelnytsky Cherkasy National University, blvd. Shevchenko 81, 18031 Cherkasy, Ukraine

S Supporting Information

ABSTRACT: An attempt was made to develop a general description of impact sensitivity. For this purpose a set of 24 well-known, as well as recently synthesized, C–H–N–O–Cl explosives covering the wide range of impact sensitivity ($h_{50} = 9–320$ cm) was studied using first-principles calculations at different external pressures. To quantify impact sensitivity, a theoretical approach was developed based on the solid-state derived criteria, which include triggering pressure, average number of electrons per atom, crystal morphology, energy content and melting temperature. These criteria follow from the theoretical consideration of the crystal compression caused by an impact event. Apart of the compression, the influence of crystal habit shapes and energy content are also discussed. The main idea is in the electron flow probability from valence to conduction bands in a solid. To support the developed theoretical background, the corresponding numerical illustration is presented in the paper. The obtained empirical correlation exhibits a significant regression coefficient ($R^2 = 0.83$). Furthermore, the found criteria have complementary character. When using them individually, the correlation becomes poor or even vanishes. Thus, a sensitive to impact explosive is expected to be more easily convertible to the metal upon compression, to possess a spherical crystal habit and to have a greater number of electrons per atom as well as a high energy content and a low melting temperature. Consequently, an insensitive explosive has the inverse characterization.



1. INTRODUCTION

The phrase “A new simple correlation...” is one of the most frequently used parts of article titles that report the study of explosives’ impact sensitivity.^{1–6} Up to now, a great variety of correlations revealed in terms of the quantitative structure–property relationships (QSPR)^{1–21} including very complex artificial neural networks (ANN)^{14–17} using different molecular features are presented in the literature. Of course we do not tend to consider this list as completely exhaustive, but it proves that QSPR is one of the most popular methodologies in predicting impact sensitivity. These QSPR models include various topological,¹⁷ electronic structure derived descriptors,^{7–13} spectral information,¹⁸ and thermodynamic¹⁹ and kinetic²⁰ criteria and often exhibit rather good correlation coefficients. This classification, however, is rather conditional since the QSPR models often include mixed descriptors.^{21,22} Generally, these QSPR studies are based on purely empirical approaches, like statistical or machine thinking methods and only a small number of works provide clear physical background for the developed correlations.^{23–27}

Meanwhile, despite the good correlation coefficients, the above-mentioned QSPR models based on the characteristics of isolated molecules cannot rationalize very simple and illustrative phenomenon, namely, polymorphism.^{28–31} It is known that different forms of explosives, for example HMX,

have different impact sensitivity.³¹ Thus, Herrmann et al.³² found that an increasing of sensitivity (up to 80%) occurs when the $\beta \rightarrow \delta$ transition in HMX takes place. The impact energies are the following: 1.96 J (β -HMX) and 0.39 J (δ -HMX), respectively. We should stress, however, that such difference although significant in practice, is small compared to sensitivity differences between distinct molecules. Another example of the shortcomings of the approach, which is based on the use of molecular characteristics, is ionic explosives. A good example of this problem is aryl diazonium salts. It is known that phenyl diazonium chloride is very sensitive explosive (impact energy 3 J),³³ but phenyl diazonium tetrafluoroborate is an extremely stable salt, which is even a commercially available reactant. Both these salts bear the same organic moiety and differ only in the nature of the anion. This means that such a big difference in impact sensitivity is hidden in the properties of the crystalline state.

Recently, we have performed a comprehensive study of these salts using first-principles calculations and revealed that most properties are rather close. Only two quantities differ significantly, namely, the pressure, which corresponds to zero

Received: February 20, 2018

Revised: May 30, 2018

Published: May 31, 2018

band gap (metallization point) and solid state enthalpy of formation (ΔH_f^0).³⁴ This study was inspired by the earlier assumption that the band gap value^{35,36} and energy storage (based on ΔH_f^0)³⁷ can be used as a criterion of impact sensitivity. Indeed, when electrons occupy conduction bands, the structure tends to decompose due to antibonding character of molecular orbitals with respect to most of the bonds. But the use of zero-pressure band gaps (ΔE_{gap}) is scarcely applicable because the values are often too large to provide an effective electron flow in the “dark” conditions.³⁸ Moreover, the divergence of the band gap values is also unacceptable; for example, monoaminotrinrobenzene (MATB) has $\Delta E_{\text{gap}} = 1.89$ eV and $h_{50} = 177$ cm, hexanitrohexaazaisowurtzitane (ϵ -CL-20) has $\Delta E_{\text{gap}} = 3.63$ eV and $h_{50} = 27$ cm, and strontium azide $\text{Sr}(\text{N}_3)_2$ has $\Delta E_{\text{gap}} = 3.71$ eV and does not explode.³⁶

On the other hand, in far 1980s, Coffey and Jacobs proposed that the key factor in initiation of explosion is the formation of so-called “hot points”, which are formed upon impact loading.³⁹ Later, it was shown that the mechanical energy can be transformed into heating by means of the phonon-to-vibrational energy transfer via the interaction of phonon overtones and vibrational fundamentals.⁴⁰ The validity of such a mechanism was recently proven for aryl diazonium salts³⁴ and several common explosives.⁴¹ Obviously, the crystal packing plays an important role in the energy dissipation due to plastic deformation and mechanical anisotropy.^{42–44}

The key moment in the initiation of the explosion is the formation of first radicals or other reactive species, which trigger the subsequent chain reaction. It is interesting that the NO_2 radical is a chain-terminating species.^{27,45} These radicals can be formed either via the transformation of the mechanical energy into heat^{46–48} or via occupation of conduction bands.³⁴ Anyway, both these processes require the crystal compression provided by an impact loading. Actually, the idea about the role of excited states in initiation of explosion was put forward long ago by Williams.⁴⁹ Later, this hypothesis was developed by Kuklja et al.,^{50–53} who studied the influence of lattice defects and shock wave on the band structure of explosives. Also, a parameter η determining the fraction of electrons promoted into virtual orbitals as a result of nonadiabatic transitions was introduced.⁵⁴ Therefore, in the present paper, we have tried to combine the factors influencing probability of the electron excitation in a crystal and subsequent propagation of explosion.

2. COMPUTATIONAL DETAILS

Density functional theory (DFT) calculations presented in this work were performed within the generalized gradient approximation (GGA). Asymmetric cell relaxations as well as the band structure calculations were carried out with the Cambridge Serial Total Energy Package (CASTEP) code⁵⁵ as implemented in the Materials Studio 7.0 program package.⁵⁶ A Vanderbilt type ultrasoft pseudopotential (USP)⁵⁷ in reciprocal space has been applied during the calculations. This allows a significant reducing of the required cutoff energy, which is useful when handling big and low-symmetry molecular systems. Note that in the present work the total number of cell relaxations and band structure calculations equals 204.

The exchange-correlation functional due to Perdew–Burke–Ernzerhof (PBE)⁵⁸ has been utilized entirely. The long-range effects were taken into account entirely using the Tkatchenko–Scheffler (TS) scheme.⁵⁹ The electronic wave functions were then expanded in a plane wave basis set with an energy cutoff equals 540 eV (39.7 Ry) for the cell relaxations and 600 eV

(44.1 Ry) for band structure calculations. Sampling of Brillouin zone was performed using k -point grids generated by the Monkhorst–Pack algorithm. Separation of k -points was set to be 0.05 \AA^{-1} for all the calculations. Convergence of the total energy was specified to 1×10^{-6} eV/atom in the SCF calculation. The rest convergence quality parameters are the following: force (0.01 eV/\AA), stress (0.02 GPa) and displacement ($5 \times 10^{-4} \text{ \AA}$).

In order to obtain crystal habits, the crystal graphs were first calculated using COMPASS⁶⁰ (Condensed-phase Optimized Molecular Potentials for Atomistic Simulation Studies) force-field within the Morphology Tools module as a part of the Materials Studio 7.0 suite of programs.⁵⁶ At the initial step, the weakest energy was specified to be $-0.596 \text{ kcal mol}^{-1}$ (thermal energy at room temperature). Then, based on the attachment energy (E_{att}) calculations, the crystal growth morphology was predicted. It is known that the crystal growth rate is proportional to E_{att} .⁶¹ Thus, the crystal growth pattern was allowed along the planes with maximum Miller indices $\{3\ 3\ 3\}$ using a Wulff plot. The attachment energy can be expressed as the energy released upon attachment of a growth slice to a crystal face eq 1:⁶¹

$$E_{\text{att}} = E_{\text{latt}} - E_{\text{slice}} \quad (1)$$

Here, E_{latt} is the crystal lattice energy; E_{slice} is the energy of a growth slice with thickness d_{hkl} .

3. RESULTS AND DISCUSSION

3.1. Theoretical Background. In the present study, we introduce three solid-state criteria of impact sensitivity, namely, triggering pressure (P_{trigg} , GPa), sphericity of crystal habits (Ψ), and the average number of electrons per atom (N_{F}). The latter parameter corresponds to integrated density of states at the Fermi level normalized to the number of atoms in asymmetric cell. Let us consider the first of them. It was proposed earlier that the electron transfer from the valence (VB) to conduction (CB) band can trigger the decomposition of the explosive.³⁶ But how can an electron overcome the big barrier, namely, the band gap (ΔE_{gap}), since the average values of the latter are about 2–3 eV? Indeed, a noticeable thermal occupation of CB is possible if ΔE_{gap} is not higher than about 1 eV.³⁸ According to the Boltzmann distribution eq 2, even in this case, the ratio of electrons in CB (\bar{n}_{CB}) and in VB (\bar{n}_{VB}) is about 10^{-17} (at 298 K) and 10^{-11} (at 500 K).

$$\frac{\bar{n}_{\text{CB}}}{\bar{n}_{\text{VB}}} = e^{-\Delta E_{\text{gap}}/kT} \quad (2)$$

It becomes clear, that the ΔE_{gap} values at zero external pressure can scarcely serve as a criterion of impact sensitivity. On the other hand, to start an explosion, a crystal requires an external stimulus which serves as a source of activation energy. Thus, the external mechanical energy (impact energy or h_{50}) must be transformed into vibrational and then into electronic energy to allow overcoming the ΔE_{gap} . Vibrational-to-electronic energy transform can proceed via the known vibronic coupling mechanism, which is essential in such nonadiabatic processes, like crystal compression. In other words, ΔE_{gap} corresponds to a part of the impact energy (or h_{50}) and can serve as the activation energy of the explosive decomposition reaction. Assuming the rate constant of explosion reaction is inversely proportional to h_{50} , one can express ΔE_{gap} as the following:⁶²

$$h_{50} \propto \frac{\prod_i^{3N-3} \nu_i^R}{\prod_i^{3N-4} \nu_i^{TS}} \exp\left(\frac{\Delta E_{\text{gap}}}{\beta_E k_B T}\right) \quad (3)$$

Here k_B is the Boltzmann constant; ν_i^R and ν_i^{TS} are the positive normal-mode frequencies of the reactant minimum and transition state, respectively.⁶² In the case of bimolecular reactions between electrophiles and nucleophiles similar approach was found to be successful;⁶³ β_E is a function, which reflects the band gap compressibility, since it is known that for most explosives the ΔE_{gap} values decreases with the rise of pressure.^{36,64} In the finite differences approximation the function β_E can be expressed as the following:

$$\frac{1}{\beta_E} = \left(\frac{P_{\text{metal}}}{\Delta E_{\text{gap}}}\right) = \tan \alpha \quad (4)$$

Here, P_{metal} is the value of external pressure corresponding to $\Delta E_{\text{gap}} = 0$ (metallic state). Thus, when a pressure becomes rise, the ΔE_{gap} value decreases gradually, and consequently, the barrier height becomes smaller and the reaction occurs faster. Since in general case the function β_E is unknown and is peculiar for each single explosive, one can use the pressure value, which corresponds to an arbitrary barrier height cutoff. We propose to use pressure at $\Delta E_{\text{gap}} = 1$ eV since below this value the thermal electron occupation of CB becomes possible; this is the so-called triggering pressure (P_{trigg}). Substituting eq 4 in eq 3 and taking into account that ΔE_{gap} is a part of the impact energy (or h_{50}), we obtain the following correlation:

$$h_{50} \propto \exp(P_{\text{trigg}}) \quad (5)$$

Recently, we have found that the metallization point (P_{metal}) values for crystalline phenyl diazonium chloride and tetrafluoroborate are 29 and 200 GPa, respectively.³⁴ Subsequently, a question then arises how such big pressures can be achievable under a standard impact testing? To answer this question, one should consider an impact event at the microscopic level. Obviously, the hammer surface has microscopic irregularities, which are the surface protrusions of different size (Figure 1a).

When a hammer edge encounters an explosive sample, only the restricted area of the hammer surface is in contact with the

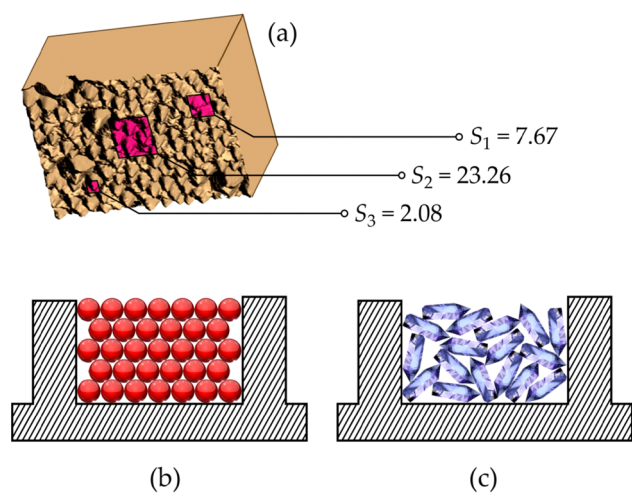


Figure 1. Representation of the hammer surface irregularities with contact zones of different relative areas (a) and packing of crystals with high (b) and low (c) sphericity.

sample. Let us call them “contact zones”; the relative areas of the three arbitrary contact zones are illustrated in Figure 1a. Since the area of a contact zone tip is actually very small, the pressure formed upon penetration of the tip into an explosive sample is expected to be extremely high (Table 1). This does

Table 1. Pressure (GPa) Formed upon the Falling of a 2.5 kg Hammer from the Determined Height (cm) with the Area of Contact Zone Being Equal To 100 μm^2

h (cm)	10	20	30	40	50	100
P (GPa)	24.5	49.1	73.6	98.1	122.6	245.3

not imply, however, that such big pressures should be achieved explicitly. Actually, electrons effectively occupy CB when the $\Delta E_{\text{gap}} = 1$ eV, which corresponds to P_{trigg} values. As a result, it does not need to compress the crystal up to the metallization point corresponding to a zero band gap value. Simultaneously, the local heating produced by the friction of the contact zone tips with the crystalline sample also facilitates the thermal excitation. As a result, the formation of first radicals or other reactive species is expected even at significantly lower pressures. Anyway, the influence of crystal compression is a crucial factor in governing impact sensitivity.

Meanwhile, if one considers VB \rightarrow CB electron transitions as a factor, which triggers decomposition of the explosive, it is useful to estimate how many electron energy levels exist below the Fermi level. Such quantity corresponds to the total number of electrons in a cell (N_F) normalized per atom and is calculated using integration of density of states.⁶⁵ The more electron energy levels exist in a solid, the more probable an electron excitation is therefore, one can write

$$h_{50} \propto 1/N_F \quad (6)$$

Now, let us discuss the influence of the crystal morphology on impact sensitivity. Since the real samples of explosives have polycrystalline form, these consist of a number of separated randomly distributed single crystals. These crystals can be agglomerated into the bigger granules or other forms (cylinders, pellets, grains, etc.). When a hammer contacts the sample, the latter undergoes an impact loading. The impact energy is spent sequentially on two processes, consolidation and compression, respectively. Until the consolidation is finished, there is no significant pressure rise in the vicinity of a contact zone. But the impact energy is spent on the friction of the crystal edges and transforms into heat.

As the crystal compression starts, the pressure rises sharply that is also accompanied by heating and change of the band structure. Thus, the ratio consolidation/compression has the influence on the position of P_{trigg} . If a sample is loose, the consolidation appears significant, but if the separated crystals are packed tightly, the crystal compression starts faster. Obviously, the crystal habit shape should influence the above-mentioned ratio (Figure 1b,c). The closer the crystal habit shape to an ideal sphere, the tighter packed the separated crystals are. A simple measure of such deviation of the shape is sphericity (Ψ), which is expressed as in eq 7.

$$\Psi = \frac{S_{\text{cryst}}}{6^{2/3} V_{\text{cryst}}^{2/3} \pi^{1/3}} \quad (7)$$

Herein, S_{cryst} and V_{cryst} are the calculated surface and volume of a crystal habit. The values which are close to a unity characterize

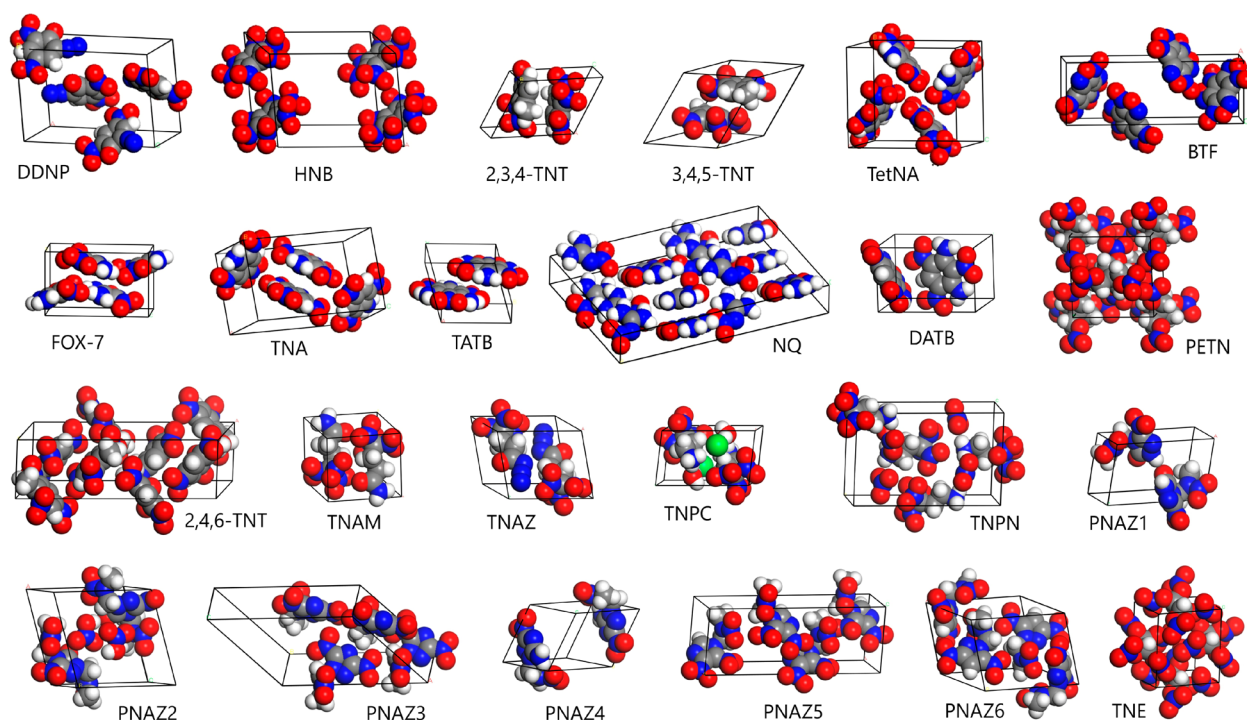


Figure 2. Chemical structures and acronyms of the studied explosives.

Table 2. Calculated and Experimental (in Parentheses) Asymmetric cell Parameters of the Studied Explosives

explosive	space group	<i>a</i> (Å)	<i>b</i> (Å)	<i>c</i> (Å)	α (deg)	β (deg)	γ (deg)	ref
DDNP	$P2_12_12_1$	6.49 (6.18)	9.08 (8.60)	15.05 (15.21)				68
HNB	$P2_1/c$	13.43 (13.22)	9.44 (9.13)	10.08 (9.68)		99.6 (95.5)		69
2,3,4-TNT	$P\bar{1}$	7.90 (7.70)	8.81 (8.33)	8.86 (8.69)	88.1 (87.9)	65.0 (65.1)	66.7 (67.3)	70
3,4,5-TNT	$P\bar{1}$	8.46 (8.33)	8.53 (8.33)	9.64 (8.75)	121.3 (155.2)	122.7 (155.2)	68.4 (70.0)	70
TetNA	$P2_1/c$	7.45 (7.27)	11.32 (11.06)	12.63 (12.27)		99.4 (98.8)		71
BTF	$Pna2_1$	7.09 (6.92)	20.24 (19.52)	6.67 (6.52)				72
FOX-7	$P2_1/c$	7.01 (6.94)	6.89 (6.57)	11.69 (11.32)		91.6 (90.6)		73
TNA	$P2_1/c$	6.23 (6.14)	9.36 (9.22)	15.61 (15.32)		99.7 (99.7)		74
TATB	$P\bar{1}$	9.17 (9.01)	9.21 (9.03)	7.13 (6.81)	109.0 (108.6)	92.1 (91.8)	119.7 (120.0)	75
NQ	$Fdd2$	18.14 (17.64)	25.63 (24.88)	3.63 (3.60)				76
DATB	Pc	7.60 (7.31)	5.32 (5.17)	12.70 (11.58)		98.01 (95.2)		77
PETN	$P\bar{4}2_1c$	10.24 (9.30)		7.02 (6.64)				78
2,4,6-TNT	$P2_1/b$	22.36 (21.41)	15.72 (15.02)	6.17 (6.09)			112.1 (111.0)	79
TNAM	$P\bar{1}$	6.28 (6.11)	7.71 (7.54)	9.23 (8.85)	78.7 (80.7)	87.5 (87.5)	87.3 (88.4)	80
TNAZ	$P\bar{1}$	7.70 (7.42)	7.77 (7.54)	9.54 (9.03)	70.5 (70.7)	79.3 (80.1)	81.8 (81.6)	80
TNPC	$P\bar{1}$	6.94 (6.74)	7.82 (7.80)	10.61 (10.07)	89.4 (90.4)	100.6 (98.8)	114.2 (114.1)	80
TNPN	$P2_12_12_1$	5.78 (5.66)	10.48 (10.28)	16.53 (16.26)				80
PNAZ1	$P2_1$	6.93 (6.76)	5.57 (5.51)	11.69 (11.39)		97.9 (97.1)		81
PNAZ2	$P2_1$	11.18 (10.83)	5.77 (5.58)	12.67 (12.36)		108.3 (107.6)		81
PNAZ3	Cc	17.99 (15.83)	7.56 (7.06)	13.54 (11.13)		136.2 (132.1)		81
PNAZ4	$P\bar{1}$	6.36 (6.30)	6.94 (6.86)	10.83 (10.63)	71.52 (72.9)	87.5 (88.0)	76.8 (77.5)	81
PNAZ5	Cc	5.86 (5.78)	21.37 (20.76)	7.84 (7.72)		93.0 (92.4)		81
PNAZ6	$P\bar{1}$	8.40 (8.23)	9.80 (9.59)	13.06 (12.79)	93.9 (93.6)	102.8 (102.9)	97.2 (96.8)	81
TNE	$P2_1/c$	8.18 (7.55)	7.53 (7.30)	9.26 (8.38)		101.7 (97.9)		82

a high sphericity, whereas a low sphericity yields the bigger values of Ψ . Thus, a sensitive explosive should have a good sphericity, which means that $h_{50} \propto \Psi$.

Finally, it is important to take into account the energy content (E_c) of an explosive, which is calculated as the heat of the decomposition reaction according to the known H_2O-CO_2 arbitrary.²² This quantity was found to correlate with $\log(h_{50})$ as well as the critical pressure of explosion initiation.⁶⁶

Recently, E_c was found to be one of the two most important sensitivity determinants for aryl diazonium salts.³⁴

3.2. Numerical Illustration. In order to provide a computational support for the above-mentioned theoretical conclusions, we have performed a series of calculations including 24 crystals. For this purpose we have selected crystalline explosives possessing relatively small molecules and covering the wide range of the h_{50} values. The asymmetric cells

of the studied explosives are illustrated in Figure 2 and their full chemical names are listed in Table S1 in the Supporting Information. The experimental (references are included in the table) and calculated unit cell parameters are listed in Table 2. As it follows from Table 2, at the USP/PBE-TS/540 eV level of theory there is a systematic overestimation of the cell volume up to 10%. Such errors are larger than typical errors obtained for molecular crystal even when thermal expansion is neglected.⁶⁷ The use of norm-conserving pseudopotentials (NCP) significantly improves the calculation results (Table S2 in the Supporting Information); however, this needs much more energy cutoff leading to huge computational cost. Therefore, we have compared band gaps obtained with USP/PBE and NCP/PBE approaches (Table S3 in the Supporting Information).

As it follows from Table S3, the differences between $\Delta E_{\text{gap}}^{\text{USP}}$ and $\Delta E_{\text{gap}}^{\text{NCP}}$ are about ± 0.056 eV, which has a negligible effect on the calculated impact sensitivity value. A similar behavior of the band gap was found when calculating the band structure on an experimental (unrelaxed) cell. For instance, in the case of 3,4,5-TNT, the ΔE_{gap} values differ only by 0.039 eV. Thus, we believe that such an overestimation of the cell volume cannot cause significant distortion of the post-SCF calculation results, since the error of the method is quenched because the same procedure is applied for all the crystals.

The effect of hydrostatic compression on the structural and electronic properties of DDNP was already studied by Gong et al.⁸³ using first-principles calculations at the local density (LDA) and generalized gradient (GGA) approximations. Their structural results at zero pressure are also close to the experimental ones; however, our presented results look better. At the LDA/CA-PZ level of theory, there were found three phase transitions at 10, 59, and 66 GPa, respectively.⁸³ In contrast, in the present work we have not detected any phase transition around 10 GPa by using the GGA/PBE-TS/540 eV approach. The molecular units remain in the form of DDNP at least to 22 GPa. Also the study of crystal compression was performed using first-principles calculations for TATB.⁸⁴ It was found that the band gap closure occurs at about 47% uniaxial strain. The metallization point for TATB was predicted to be 120 GPa.⁸⁴ In the present study we predict this value at about 140 GPa.

The calculated band gaps of the studied crystalline explosives are gathered in Table 3 and the corresponding BS plots are illustrated in Figure S1 in the Supporting Information. As one can see in Table 3, the ΔE_{gap} values vary in a rather wide range (1–4 eV). We should stress, however, that the BS calculations have been performed using pure GGA functional PBE, which usually underestimate the ΔE_{gap} values. Much closer to the experimental ones are the band gap values, which are obtained when using hybrid exchange-correlation functionals, in particular, HSE06.⁸⁵ Recently we have found that the PBE values are about 50–60% from that of HSE06.^{86,87} Despite the lower band gap values, the use of PBE functional is reasonable because we use the same approach for all the crystals; therefore, the obtained trend remains unchanged. Along with the band gap values, we have calculated integrated densities of states for the studied explosives. The corresponding plots are illustrated in Figure S2 in the Supporting Information. At the Fermi level this corresponds to the total number of electrons in a cell. Note that in the pseudopotential method only valence electrons should be taken into account. Herein, valence electrons are the

Table 3. Electronic Properties of the Studied Explosives

explosive	ΔE_{gap}	gap	VBM	CBM
DDNP	2.021	indirect	Γ	Y
HNB	2.447	indirect	A	Γ
2,3,4-TNT	2.699	indirect	Z	F
3,4,5-TNT	2.380	indirect	Q	Γ
TetNA	1.877	indirect	Γ	C
BTF	2.205	indirect	U	Γ
FOX-7	2.220	indirect	D	E
TNA	1.953	direct	Γ	Γ
TATB	2.430	indirect	Z	Q
NQ	3.350	direct	Γ	Γ
DATB	2.169	direct	Γ	Γ
PETN	3.993	direct	Γ	Γ
2,4,6-TNT	3.155	direct	Γ	Γ
TNAM	1.480	direct	Γ	Γ
TNAZ	2.208	indirect	Z	F
TNPC	2.098	indirect	Γ	Q
TNPN	1.047	direct	Γ	Γ
PNAZ1	2.060	direct	B	B
PNAZ2	2.242	indirect	D	A
PNAZ3	2.346	indirect	L	A
PNAZ4	1.665	indirect	Z	F
PNAZ5	2.166	indirect	M	L
PNAZ6	2.537	direct	F	F
TNE	4.289	direct	G	G

following: $2s^2 2p^2$ for carbon, $1s^1$ for hydrogen, $2s^2 2p^3$ for nitrogen, $2s^2 2p^4$ for oxygen and $3s^2 3p^5$ for chlorine.

A comparison of several experimentally available crystal habits^{82,88–90} with the predicted ones is presented in Figure 3.

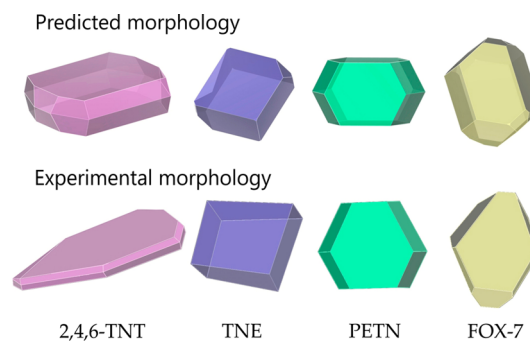


Figure 3. Comparison of the calculated and experimental crystal habits for several explosives.

All the rest of the calculated habits are illustrated in Figure S3 in the Supporting Information. Of course, the predicted morphology in vacuum can differ significantly from that obtained after recrystallization from a certain solvent. To improve results, one should apply the recently developed modified attachment energy method (MAE), which allows the crystal morphology after recrystallization to be calculated.⁹¹

The search of triggering pressure is the most computationally expensive procedure within this study. Ideally, one must perform three trials to detect P_{trigg} but this is possible only when the function β_E has strictly linear character. The latter, however, often is only close to linear (Figure 4, FOX-7); otherwise, the number of trials rises (Figure 4, TATB). For the rest of the explosives, the plots of band gaps versus pressure are presented in Figure S4 in the Supporting Information.

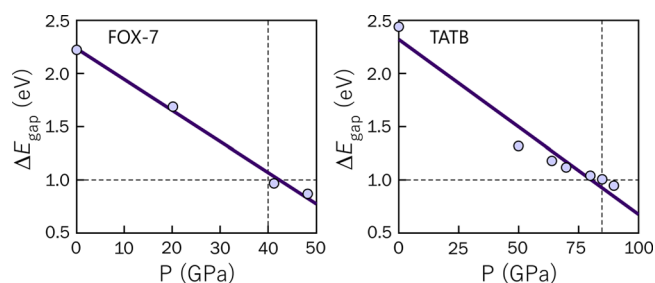


Figure 4. Band gap as a linear (FOX-7) and nonlinear (TATB) function of hydrostatic compression.

Additionally, the calculation schemes of E_c together with experimental standard solid-state enthalpies of formation are listed in Table S4 in the [Supporting Information](#).

The numerical values of P_{trigg} , N_F , Ψ , and E_c along with the experimental values of h_{50} are listed in Table 4. We should stress that the values of impact energy (in J) from refs 80–82 were converted into impact heights (in cm) in order to align these data with the previous sets from refs 12 and 92. As one can see in Table 4, there is a noticeable correlation of the N_F vs h_{50} values; the correlation coefficient R^2 is 0.39 (see Figure S5 in the [Supporting Information](#)). Apart from the N_F values, the E_c and P_{trigg} quantities also demonstrate trends which are predicted in the previous section, but the R^2 values are unacceptable. Moreover, a simple correlation of h_{50} with the ΔE_{gap} values completely fails (Figure S5 in the [Supporting Information](#)).

As a result, we have combined these four quantities together in order to find a more accurate empirical correlation. For this purpose we have also added melting point T_m (K). The origin of this correction comes from local heating of a crystal

undergoing compression. Indeed, the free radicals or other reactive species formed upon breaking of the trigger bonds can initiate further decomposition only in the liquid or gaseous state. Thus, in the vicinity of a contact zone the crystal should at least melt. This means that the low-melting crystals should be more sensitive than the high-melting ones or simply $h_{50} \propto T_m$. The T_m values are listed in Table S5 in the [Supporting Information](#). In this approach, the obtained correlation produces the complex sensitivity function Ω , which can be expressed as in eq 8:

$$\Omega = \frac{\Psi T_m^2}{N_F^7} \exp\left(\frac{P_{trigg}}{1000}\right) \exp\left(\frac{E_c}{100}\right) \quad (8)$$

Remarkably, the correlation of Ω and h_{50} is much better with the correlation coefficient $R^2 = 0.83$.

As one can see in Figure S5, the correlation of zero band gaps exhibits a similar R^2 value with the same correlation of P_{trigg} values. We should stress, however, that the P_{trigg} values for PETN, TNAZ and TNE poorly fits the general trend (Figure S5 in the [Supporting Information](#)). After removing these values from the correlation the resulting R^2 becomes 0.34. In contrast, the ΔE_{gap} values exhibit a uniform dispersion. The correlation of Ω with the experimental h_{50} values is presented graphically in Figure 5. On the basis of Ω values we have obtained theoretical impact sensitivities (h_{50}^{theor}), which can be simply calculated using the following regression equation:

$$h_{50}^{theor} = 5.018\Omega - 36.860 \quad (9)$$

For the correlation of h_{50}^{theor} and h_{50}^{exper} we have calculated several statistical functions including standard deviation (SD), median (Me), and confidence interval at 99% probability; these are presented in Figure 5.

Table 4. Calculated data on predicting impact sensitivity

explosive	h_{50} (cm)	Ψ	P_{trigg} (GPa)	N_F (\bar{v} atom $^{-1}$)	E_c (kJ mol $^{-1}$ atom $^{-1}$)	Ω
DDNP	9 ^a	1.139	22	4.47	81.99	13.695
HNB	11 ^a	1.248	20	5.25	112.72	10.005
2,3,4-TNT	56 ^a	1.140	50	3.79	60.90	29.104
3,4,5-TNT	107 ^a	1.191	40	4.00	60.48	23.399
TetNA	47 ^a	1.248	29	4.55	77.09	16.497
BTF	53 ^a	1.230	105	5.00	99.25	10.334
FOX-7	126 ^b	1.132	40	4.00	38.97	27.727
TNA	141 ^a	1.179	37	4.20	64.29	21.452
TATB	200 ^a	1.146	86	4.00	50.59	49.066
NQ	320 ^b	1.230	121	3.64	43.10	64.795
DATB	200 ^a	1.231	30	4.09	59.33	37.146
2,4,6-TNT	98 ^a	1.439	82	4.00	63.81	22.487
PETN	16 ^b	1.154	198	4.14	75.13	24.604
TNAM	40 ^c	1.263	90	4.00	62.79	21.169
TNAZ	13 ^c	1.261	150	4.38	76.64	8.859
TNPC	131 ^c	1.239	100	3.90	60.17	34.012
TNPN	40 ^c	1.193	1	4.08	79.73	23.311
PNAZ1	66 ^d	1.332	75	3.90	56.19	32.710
PNAZ2	265 ^d	1.288	200	3.74	57.15	63.531
PNAZ3	46 ^d	1.132	72	4.16	73.60	22.597
PNAZ4	265 ^d	1.184	80	3.73	54.72	54.790
PNAZ5	165 ^d	1.215	100	4.00	66.86	34.285
PNAZ6	125 ^d	1.221	60	4.00	67.77	36.356
TNE	13 ^e	1.273	154	5.10	34.41	3.076

^aReference 92. ^bReference 12. ^cConverted from ref 80. ^dConverted from ref 81. ^eConverted from ref 82.

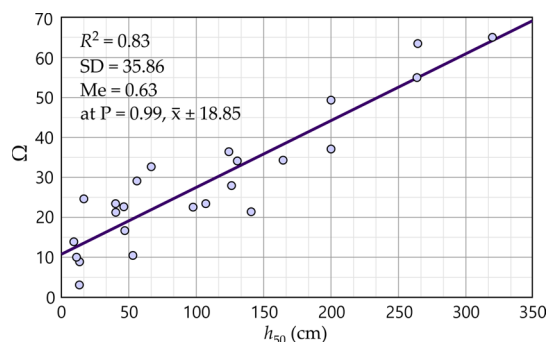


Figure 5. Plot of sensitivity parameter Ω as a function of the experimental h_{50} values.

4. CONCLUSIONS

Summing up, we have considered impact sensitivity as a complex phenomenon with stochastic character, which cannot be simply described by an arbitrary empirical correlation. Meanwhile, a few solid-state parameters have been clearly shown as functions of impact sensitivity. We speculate that the developed approach can be extrapolated to other families of explosives, not just for the aromatic, aliphatic, and heterocyclic nitro and nitrate compounds studied in this work.

Thus, conception of the thermal electron excitation, which was effectively applied earlier for the reactions between nucleophiles and electrophiles, now involves initiation of detonation in solids. Surprisingly, these seemingly completely different types of reactions have similar features. In both these types, the key point is the electronically excited state of a molecule or molecular complex. Therefore, the problem of initiation of detonation becomes the problem of thermal electron excitation. In the present paper, we have described how to reach these excited states using mechanical energy. It is probable that the other kinds of sensitivity (shock, spark, etc.) have a similar nature but differ only in the mechanisms of energy transformation allowing electron excitation.

Computationally, the search of triggering pressure is rather expensive and requires a few trials; therefore, an alternative method for searching the P_{trigg} values would be very useful. In this context, the most promising method is one based on elastic constants calculation. Indeed, with rare exceptions, one can consider band gap compressibility as a linear function of pressure. As a result, one can suggest using bulk modulus instead of triggering pressure. This method is expected to be simpler and faster; thus, it will be the topic of a further, more detailed study.

■ ASSOCIATED CONTENT

Supporting Information

The Supporting Information is available free of charge on the ACS Publications website at DOI: 10.1021/acs.jpca.8b01743.

Structural data, estimation errors, band structures and partial density of states plots, integrated density of states, crystal habits, and melting temperatures (PDF)

■ AUTHOR INFORMATION

Corresponding Author

*Fax: (+3) 80472 37-21-42. Telephone: (+3) 80472 37-65-76.

E-mail: bondchem@cdu.edu.ua.

ORCID

Sergey V. Bondarchuk: 0000-0002-3545-0736

Notes

The author declares no competing financial interest.

■ ACKNOWLEDGMENTS

This work was supported by the Ministry of Education and Science of Ukraine, Research Fund (Grant No. 0117U003908).

■ REFERENCES

- (1) Keshavarz, M. H. A New General Correlation for Predicting Impact Sensitivity of Energetic Compounds. *Propellants, Explos., Pyrotech.* **2013**, *38*, 754–760.
- (2) Keshavarz, M. H.; Pouretedal, H. R.; Semnani, A. Novel Correlation for Predicting Impact Sensitivity of Nitroheterocyclic Energetic Molecules. *J. Hazard. Mater.* **2007**, *141*, 803–807.
- (3) Keshavarz, M. H.; Zali, A.; Shokrolahi, A. A Simple Approach for Predicting Impact Sensitivity of Polynitroheteroarenes. *J. Hazard. Mater.* **2009**, *166*, 1115–1119.
- (4) Keshavarz, M. H. Simple Relationship for Predicting Impact Sensitivity of Nitroaromatics, Nitramines, and Nitroaliphatics. *Propellants, Explos., Pyrotech.* **2010**, *35*, 175–181.
- (5) Fayet, G.; Rotureau, P. Development of Simple QSPR Models for the Impact Sensitivity of Nitramines. *J. Loss Prev. Process Ind.* **2014**, *30*, 1–8.
- (6) Keshavarz, M. H.; Pouretedal, H. R. Simple Empirical Method for Prediction of Impact Sensitivity of Selected Class of Explosives. *J. Hazard. Mater.* **2005**, *124*, 27–33.
- (7) Shuo, G. QSPR Studies on Impact Sensitivities of High Energy Density Molecules. *Adv. Mater. Res.* **2013**, *641–642*, 109–112.
- (8) Rice, B. M.; Hare, J. J. A Quantum Mechanical Investigation of the Relation between Impact Sensitivity and the Charge Distribution in Energetic Molecules. *J. Phys. Chem. A* **2002**, *106*, 1770–1783.
- (9) Politzer, P.; Lane, P.; Murray, J. S. Sensitivities of Ionic Explosives. *Mol. Phys.* **2017**, *115*, 497–509.
- (10) David Stephen, A.; Srinivasan, P.; Kumaradhas, P. Bond Charge Depletion, Bond Strength and the Impact Sensitivity of High Energetic 1,3,5-Triamino 2,4,6-Trinitrobenzene (TATB) Molecule: A Theoretical Charge Density Analysis. *Comput. Theor. Chem.* **2011**, *967*, 250–256.
- (11) Murray, J. S.; Concha, M. C.; Politzer, P. Links Between Surface Electrostatic Potentials of Energetic Molecules, Impact Sensitivities and C–NO₂/N–NO₂ Bond Dissociation Energies. *Mol. Phys.* **2009**, *107*, 89–97.
- (12) Pospíšil, M.; Vávra, P.; Concha, M. C.; Murray, J. S.; Politzer, P. A Possible Crystal Volume Factor in the Impact Sensitivities of Some Energetic Compounds. *J. Mol. Model.* **2010**, *16*, 895–901.
- (13) Chaoyang, Z.; Yuanjie, S.; Yigang, H.; Xinfeng, W. Theoretical Investigation of the Relationship between Impact Sensitivity and the Charges of the Nitro Group in Nitro Compounds. *J. Energ. Mater.* **2005**, *23*, 107–119.
- (14) Nefati, H.; Cense, J.-M.; Legendre, J.-J. Prediction of the Impact Sensitivity by Neural Networks. *J. Chem. Inf. Comput. Sci.* **1996**, *36*, 804–810.
- (15) Keshavarz, M. H.; Jaafari, M. Investigation of the Various Structure Parameters for Predicting Impact Sensitivity of Energetic Molecules via Artificial Neural Network. *Propellants, Explos., Pyrotech.* **2006**, *31*, 216–225.
- (16) Wang, R.; Jiang, J.; Pan, Y. Prediction of Impact Sensitivity of Nonheterocyclic Nitroenergetic Compounds Using Genetic Algorithm and Artificial Neural Network. *J. Energ. Mater.* **2012**, *30*, 135–155.
- (17) Wang, R.; Jiang, J.; Pan, Y.; Cao, H.; Cui, Y. Prediction of Impact Sensitivity of Nitro Energetic Compounds by Neural Network Based on Electrotological-State Indices. *J. Hazard. Mater.* **2009**, *166*, 155–186.
- (18) Jungová, M.; Zeman, S.; Yan, Q.-L. Recent Advances in the Study of the Initiation of Nitramines by Impact Using Their ¹⁵N NMR Chemical Shifts. *Cent. Eur. J. Energ. Mater.* **2014**, *11*, 383–393.

- (19) Vaullerlin, M.; Espagnacq, A.; Morin-Allory, L. Prediction of Explosives Impact Sensitivity. *Propellants, Explos., Pyrotech.* **1998**, *23*, 237–239.
- (20) Chen, Z.-X.; Xiao, H. Impact Sensitivity and Activation Energy of Pyrolysis for Tetrazole Compounds. *Int. J. Quantum Chem.* **2000**, *79*, 350–357.
- (21) Yan, Q.-L.; Zeman, S. Theoretical Evaluation of Sensitivity and Thermal Stability for High Explosives Based on Quantum Chemistry Methods: A Brief Review. *Int. J. Quantum Chem.* **2013**, *113*, 1049–1061.
- (22) Mathieu, M. Sensitivity of Energetic Materials: Theoretical Relationships to Detonation Performance and Molecular Structure. *Ind. Eng. Chem. Res.* **2017**, *56*, 8191–8201.
- (23) Mathieu, D.; Alaime, T. Impact Sensitivities of Energetic Materials: Exploring the Limitations of a Model Based only on Structural Formulas. *J. Mol. Graphics Modell.* **2015**, *62*, 81–86.
- (24) Mathieu, D. Toward a Physically Based Quantitative Modeling of Impact Sensitivities. *J. Phys. Chem. A* **2013**, *117*, 2253–2259.
- (25) Mathieu, D.; Alaime, T. Predicting Impact Sensitivities of Nitro Compounds on the Basis of a Semi-Empirical Rate Constant. *J. Phys. Chem. A* **2014**, *118*, 9720–9726.
- (26) Chen, Z.-X.; Xiao, H.-M. Quantum Chemistry Derived Criteria for Impact Sensitivity. *Propellants, Explos., Pyrotech.* **2014**, *39*, 487–495.
- (27) Rice, B. M.; Sahu, S.; Owens, F. J. Density functional calculations of bond dissociation energies for NO₂ scission in some nitroaromatic molecules. *J. Mol. Struct.: THEOCHEM* **2002**, *583*, 69–72.
- (28) Millar, D. I. A.; Oswald, I. D. H.; Francis, D. J.; Marshall, W. J.; Pulham, C. R.; Cumming, A. S. The Crystal Structure of β -RDX—an Elusive Form Of an Explosive Revealed. *Chem. Commun.* **2009**, 562–564.
- (29) Davidson, A. J.; Oswald, I. D. H.; Francis, D. J.; Lennie, A. R.; Marshall, W. J.; Millar, D. I. A.; Pulham, C. R.; Warren, J. E.; Cumming, A. S. Explosives Under Pressure—the Crystal Structure of γ -RDX as Determined by High-Pressure X-Ray and Neutron Diffraction. *CrystEngComm* **2008**, *10*, 162–165.
- (30) Peng, Q.; Rahul, Wang, G.; Liu, G.-R.; De, S. Structures, Mechanical Properties, Equations of State, And Electronic Properties of β -HMX under Hydrostatic Pressures: a DFT-D2 Study. *Phys. Chem. Chem. Phys.* **2014**, *16*, 19972–19983.
- (31) Asay, B. W.; Henson, B. F.; Smilowitz, L. B.; Dickson, P. M. On the Difference in Impact Sensitivity of Beta and Delta HMX. *J. Energ. Mater.* **2003**, *21*, 223–235.
- (32) Herrmann, M.; Engel, W.; Eisenreich, N. Thermal Expansion, Transitions, Sensitivities and Burning Rates of HMX. *Propellants, Explos., Pyrotech.* **1992**, *17*, 190–195.
- (33) Ullrich, R.; Grewer, T. Decomposition of Aromatic Diazonium Compounds. *Thermochim. Acta* **1993**, *225*, 201–211.
- (34) Bondarchuk, S. V. Impact Sensitivity of Crystalline Phenyl Diazonium Salts: a First-Principles Study of Solid-State Properties Determining the Phenomenon. *Int. J. Quantum Chem.* **2017**, *117*, e25430.
- (35) Zhang, H.; Cheung, F.; Zhao, F.; Cheng, X.-L. Band Gaps and the Possible Effect on Impact Sensitivity for Some Nitro Aromatic Explosive Materials. *Int. J. Quantum Chem.* **2009**, *109*, 1547–1552.
- (36) Zhu, W.; Xiao, H. First-Principles Band Gap Criterion for Impact Sensitivity of Energetic Crystals: a Review. *Struct. Chem.* **2010**, *21*, 657–665.
- (37) Fried, L. E.; Manaa, M. R.; Pagoria, P. F.; Simpson, R. L. Design and Synthesis of Energetic Materials. *Annu. Rev. Mater. Res.* **2001**, *31*, 291–321.
- (38) Bondarchuk, S. V.; Minaev, B. F. Thermally Accessible Triplet State of π -Nucleophiles does Exist. Evidence from First Principles Study of Ethylene Interaction with Copper Species. *RSC Adv.* **2015**, *5*, 11558–11569.
- (39) Coffey, C. S.; Jacobs, S. J. Detection of Local Heating in Impact or Shock Experiments with Thermally Sensitive Films. *J. Appl. Phys.* **1981**, *52*, 6991–6993.
- (40) McNesby, K. L.; Coffey, C. S. Spectroscopic Determination of Impact Sensitivities of Explosives. *J. Phys. Chem. B* **1997**, *101*, 3097–3104.
- (41) Bernstein, J. Ab initio study of energy transfer rates and impact sensitivities of crystalline explosives. *J. Chem. Phys.* **2018**, *148*, 084502.
- (42) Ma, Y.; Zhang, A.; Xue, X.; Jiang, D.; Zhu, Y.; Zhang, C. Crystal Packing of Impact-Sensitive High-Energy Explosives. *Cryst. Growth Des.* **2014**, *14*, 6101–6114.
- (43) An, Q.; Cheng, T.; Goddard, W. A., III; Zybin, S. V. Anisotropic Impact Sensitivity and Shock Induced Plasticity of TKX-50 (Dihydroxylammonium 5,5'-Bis(tetrazole)-1,1'-diolate) Single Crystals: from Large-Scale Molecular Dynamics Simulations. *J. Phys. Chem. C* **2015**, *119*, 2196–2207.
- (44) Jones, T. E. Role of Inter- and Intramolecular Bonding on Impact Sensitivity. *J. Phys. Chem. A* **2012**, *116*, 11008–11014.
- (45) Miles, M. H.; DeVries, K. L.; Britt, A. D.; Moniz, W. B. Impact Sensitivity of γ -Irradiated HMX. *Propellants, Explos., Pyrotech.* **1983**, *8*, 49–52.
- (46) Wu, Y.-Q.; Huang, F.-L.; Zhang, Z.-Y. Experiments and Modeling of HMX Granular Explosives Subjected to Drop-Weight Impact. *RSC Adv.* **2012**, *2*, 4152–4163.
- (47) Dubovik, A. V. Approximate Method for Calculating the Impact Sensitivity Indices of Solid Explosive Mixtures. *Combust., Explos. Shock Waves* **2001**, *37*, 99–105.
- (48) Zhang, G.; Weeks, B. L. A Device for Testing Thermal Impact Sensitivity of High Explosives. *Propellants, Explos., Pyrotech.* **2010**, *35*, 440–445.
- (49) Williams, F. Electronic states of solid explosives and their probable role in detonations. *Adv. Chem. Phys.* **2007**, *21*, 289–302.
- (50) Kuklja, M. M. On the initiation of chemical reactions by electronic excitations in molecular solids. *Appl. Phys. A: Mater. Sci. Process.* **2003**, *76*, 359–366.
- (51) Kuklja, M. M.; Aduiev, B. P.; Aluker, E. D.; Krashenin, V. I.; Krechetov, A. G.; Mitrofanov, A. Yu. Role of electronic excitations in explosive decomposition of solids. *J. Appl. Phys.* **2001**, *89*, 4156.
- (52) Kuklja, M. M.; Rashkeev, S. N.; Zerilli, F. J. Shear-strain induced decomposition of 1,1-diamino-2,2-dinitroethylene. *Appl. Phys. Lett.* **2006**, *89*, 071904.
- (53) Tsyshkevsky, R. V.; Sharia, O.; Kuklja, M. M. Molecular Theory of Detonation Initiation: Insight from First Principles Modeling of the Decomposition Mechanisms of Organic Nitro Energetic Materials. *Molecules* **2016**, *21*, 236.
- (54) Mathieu, D.; Martin, P.; La Hargue, J.-P. Simulation of the Electron Dynamics in Shockwaves and Implications for the Sensitivity of Energetic Materials. *Phys. Scr.* **2005**, *118*, 171–173.
- (55) Clark, S. J.; Segall, M. D.; Pickard, C. J.; Hasniz, P. J.; Probert, M. J.; Refson, K.; Payne, M. C. First Principles Methods Using CASTEP. *Z. Kristallogr. - Cryst. Mater.* **2005**, *220*, 567–570.
- (56) *Materials Studio 7.0*; Accelrys, Inc.: San Diego, CA, 2013.
- (57) Vanderbilt, D. Soft Self-Consistent Pseudopotentials in a Generalized Eigenvalue Formalism. *Phys. Rev. B: Condens. Matter Mater. Phys.* **1990**, *41*, 7892–7895.
- (58) Perdew, J. P.; Burke, K.; Ernzerhof, M. Generalized Gradient Approximation Made Simple. *Phys. Rev. Lett.* **1996**, *77*, 3865–3868.
- (59) Tkatchenko, A.; Scheffler, M. Accurate Molecular Van Der Waals Interactions from Ground-State Electron Density and Free-Atom Reference Data. *Phys. Rev. Lett.* **2009**, *102*, 073005.
- (60) Sun, H. COMPASS: An ab Initio Force-Field Optimized for Condensed-Phase Applications – Overview with Details on Alkane and Benzene Compounds. *J. Phys. Chem. B* **1998**, *102*, 7338–7364.
- (61) Berkovitch-Yellin, Z. Toward an Ab Initio Derivation Of Crystal Morphology. *J. Am. Chem. Soc.* **1985**, *107*, 8239–8253.
- (62) Voter, A. F. Introduction to the kinetic Monte Carlo method. *Radiation Effects in Solids* **2007**, *235*, 1–23.
- (63) Bondarchuk, S. V.; Minaev, B. F. The Singlet-Triplet Energy Splitting Of π -Nucleophiles as a Measure of their Reaction Rate with Electrophilic Partners. *Chem. Phys. Lett.* **2014**, *607*, 75–80.
- (64) Fedorov, I. A.; Fedorova, T. P.; Zhuravlev, Y. N. Hydrostatic Pressure Effects on Structural and Electronic Properties of ETN and

PETN from First Principles Calculations. *J. Phys. Chem. A* **2016**, *120*, 3710–3717.

(65) Veselić, I. Existence of the Integrated Density of States. In *Existence and Regularity Properties of the Integrated Density of States of Random Schrödinger Operators*; Veselić, I., Ed.; Springer: Berlin, 2008; pp 13–43.

(66) Pepekin, V. I.; Korsunskii, B. L.; Denisaev, A. A. Initiation of Solid Explosives by Mechanical Impact. *Combust., Explos. Shock Waves* **2008**, *44*, 586–590.

(67) Balu, R.; Byrd, E. F. C.; Rice, B. M. Assessment of Dispersion Corrected Atom Centered Pseudopotentials: Application to Energetic Molecular Crystals. *J. Phys. Chem. B* **2011**, *115*, 803–810.

(68) Lowe-Ma, C. K.; Nissan, R. A.; Wilson, W. S.; Houk, K. H.; Wang, X. B. Structure of Diazophenols: Crystal Structure, ^{13}C N.M.R. Spectroscopy, and Molecular Orbital Studies. *J. Chem. Res.* **1988**, 1740–1756.

(69) Akopyan, Z. A.; Struchkov, Y. T.; Dashevskii, V. G. Crystal and Molecular Structure of Hexanitrobenzene. *J. Struct. Chem.* **1967**, *7*, 385–392.

(70) Demartin, F.; Filippini, G.; Gavezzotti, A.; Rizzato, S. X-Ray Diffraction and Packing Analysis on Vintage Crystals: Wilhelm Koerner's Nitrobenzene Derivatives from the School of Agricultural Sciences in Milano. *Acta Crystallogr., Sect. B: Struct. Sci.* **2004**, *B60*, 609–620.

(71) Dickinson, C.; Stewart, J. M.; Holden, J. R. A Direct Determination of the Crystal Structure of 2,3,4,6-Tetranitroaniline. *Acta Crystallogr.* **1966**, *21*, 663–670.

(72) Golovina, N. I.; Titkov, A. N.; Raevskii, A. V.; Atovmyan, L. O. Kinetics and Mechanism of Phase Transitions in the Crystals of 2,4,6-Trinitrotoluene and Benzotrifuroxane. *J. Solid State Chem.* **1994**, *113*, 229–238.

(73) Bemm, U.; Östmark, H. 1,1-Diamino-2,2-dinitroethylene: a Novel Energetic Material with Infinite Layers in Two Dimensions. *Acta Crystallogr., Sect. C: Cryst. Struct. Commun.* **1998**, *C54*, 1997–1999.

(74) Holden, J. R.; Dickinson, C.; Bock, C. M. Crystal Structure of 2,4,6-Trinitroaniline. *J. Phys. Chem.* **1972**, *76*, 3597–3602.

(75) Cady, H. H.; Larson, A. C. The Crystal Structure of 1,3,5-Triamino-2,4,6-trinitrobenzene. *Acta Crystallogr.* **1965**, *18*, 485–496.

(76) Choi, C. S. Refinement of 2-Nitroguanidine by Neutron Powder Diffraction. *Acta Crystallogr., Sect. B: Struct. Crystallogr. Cryst. Chem.* **1981**, *B37*, 1955–1957.

(77) Holden, J. R. The Structure of 1,3-Diamino-2,4,6-trinitrobenzene, Form I. *Acta Crystallogr.* **1967**, *22*, 545–550.

(78) Booth, A. D.; Llewellyn, F. J. The crystal structure of pentaerythritol tetranitrate. *J. Chem. Soc.* **1947**, 837–846.

(79) Golovina, N. I.; Titkov, A. N.; Raevskii, A. V.; Atovmyan, L. O. Kinetics and Mechanism of Phase Transitions in the Crystals of 2,4,6-Trinitrotoluene and Benzotrifuroxane. *J. Solid State Chem.* **1994**, *113*, 229–238.

(80) Axthammer, Q. J.; Klapötke, T. M.; Krumm, B.; Scharf, R.; Unger, C. C. Convenient synthesis of energetic polynitro materials including $(\text{NO}_2)_3\text{CCH}_2\text{CH}_2\text{NH}_3$ -salts via Michael addition of trinitromethane. *Dalton Trans.* **2016**, *45*, 18909–18920.

(81) Klapötke, T. M.; Pengler, A.; Pflüger, C.; Stierstorfer, J. Melt-cast materials: combining the advantages of highly nitrated azoles and open-chain nitramines. *New J. Chem.* **2016**, *40*, 6059–6069.

(82) Fischer, D.; Klapötke, T. M.; Stierstorfer, J. Tetranitrateoethane. *Chem. Commun.* **2016**, *52*, 916–918.

(83) Liu, Y.; Gong, X.; Wang, L.; Wang, G. Effect of Hydrostatic Compression on Structure and Properties of 2-Diazo-4,6-Dinitrophenol Crystal: Density Functional Theory Studies. *J. Phys. Chem. C* **2011**, *115*, 11738–11748.

(84) Wu, C. J.; Yang, L. H.; Fried, L. E.; et al. Electronic Structure of Solid 1,3,5-Triamino-2,4,6-trinitrobenzene under Uniaxial Compression: Possible Role of Pressure-Induced Metallization in Energetic Materials. *Phys. Rev. B: Condens. Matter Mater. Phys.* **2003**, *67*, 235101.

(85) Dongho Nguimdo, G. M.; Joubert, D. P. A Density Functional (PBE, PBEsol, HSE06) Study of the Structural, Electronic and Optical

Properties of the Ternary Compounds AgAlX_2 ($X = \text{S}, \text{Se}, \text{Te}$). *Eur. Phys. J. B* **2015**, *88*, 113–123.

(86) Bondarchuk, S. V.; Minaev, B. F. Super High-Energy Density Single-Bonded Trigonal Nitrogen Allotrope—a Chemical Twin of the Cubic Gauche form of Nitrogen. *Phys. Chem. Chem. Phys.* **2017**, *19*, 6698–6706.

(87) Bondarchuk, S. V.; Minaev, B. F. DFT Design of Polyguanidine – a Unique Two-Dimensional Material with High-Energy Density. *Mol. Phys.* **2017**, *115*, 2423–2430.

(88) Gallagher, H. G.; Vrcelj, R. M.; Sherwood, J. N. The crystal growth and perfection of 2,4,6-trinitrotoluene. *J. Cryst. Growth* **2003**, *250*, 486–498.

(89) Hikal, W. M.; Bhattacharia, S. K.; Peterson, G. R.; Weeks, B. L. Controlling the coarsening stability of pentaerythritol tetranitrate (PETN) single crystals by the use of water. *Thermochim. Acta* **2012**, *536*, 63–67.

(90) Trzcíński, W. A.; Cudziło, S.; Chylek, Z.; Szymańczyk, L. Detonation properties of 1,1-diamino-2,2-dinitroethene (DADNE). *J. Hazard. Mater.* **2008**, *157*, 605–612.

(91) Liu, N.; Li, Y.-N.; Zeman, S.; Shu, Y.-J.; Wang, B.-Z.; Zhou, Y.-S.; Zhao, Q.-L.; Wang, W.-L. The crystal morphology of 3,4-bis(3-nitrofurazan-4-yl)furoxan (DNTF) in the solvent system: Molecular dynamics simulation and sensitivity study. *CrystEngComm* **2016**, *18*, 2843–2851.

(92) Wilson, W. S.; Bliss, D. E.; Christian, S. L.; Knight, D. J. *Explosive Properties of Polynitroaromatics*, NWC/TP-7073; Naval Weapons Center: China Lake, CA, 1990.